Temporal variability of dissolved trace metals at the DYFAMED time-series station, Northwestern Mediterranean

Christophe Migon, Lars-Eric Heimbürger-Boavida, Aurélie Dufour, Jean-François Chiffoleau, Daniel Cossa

Temporal variability of dissolved trace metals at the DYFAMED time-series station, Northwestern Mediterranean

Christophe Migon[a*], Lars-Eric Heimbürger-Boavida[a,b,c], Aurélie Dufour[a,c], Jean-François Chiffoleau[d], and Daniel Cossa[b, e]

[a]*Sorbonne Université, CNRS/INSU, Laboratoire d'Océanographie de Villefranche-sur-Mer, F-06234, Villefranche-sur-Mer, France*

[b]*Ifremer, Centre de Méditerranée, BP 330, F-83507 La Seyne-sur-Mer, France*

[c]*Aix-Marseille Université, CNRS/INSU, Université de Toulon, IRD, Mediterranean Institute of Oceanography (MIO), UM 110, F-13288 Marseille, France*

[d]*Ifremer, Centre Atlantique, BP 21105, F-44311 Nantes Cedex 03, France*

[e]*Université Grenoble Alpes, ISTerre, BP 53, F-38041 Grenoble, France*

**Corresponding author*

migon@obs-vlfr.fr

Tel: +33 4 93 76 39 90

Fax: +33 4 93 76 37 39

Highlights

- We sort out the influence of these different parameters in the water column in a low-nutrient low-chlorophyll region, the Ligurian sea (Western Mediterranean);
- The intensity of winter mixing determines the homogenization of TM concentrations in the water column;

- TM exhibit a range of biogeochemical behaviours from surface-enriched (scavenged-type) to surface-depleted (nutrient-like) with Co and Ni as representative cases;
- Atmospheric input is a chief parameter as is determine Pb, Cu and Co distributions, and preclude any limitation of primary production by TM;
- Anthropogenic Pb decreased by up to 60% and 20% in surface and deep waters the last 20 years, but water column is still Pb contaminated, in such a way that the Western Mediterranean deep-water outflow is the source of Pb contamination observed at 1000m in the adjacent Eastern North Atlantic Ocean.

Abstract

We present here results of an 18-month survey (July 2007-March 2009) of a suite of selected trace metals (TM: Co, Ni, Cu, Pb) in a 2350 m-deep offshore water column in the Ligurian Sea (Northwestern Mediterranean Sea). This low-nutrient low-chlorophyll region is characterised by a long stratification period (May-November) during which surface waters are depleted of macronutrients. Trace metals exhibit a range of biogeochemical behaviours from surface-enriched (scavenged-type) to surface-depleted (nutrient-like) with Co and Ni as representative cases. Cobalt (28 - 172 pM) distributions are governed by external inputs of aeolian dust deposition and removal by adsorption onto particles in surface, intermediate and deep waters as well. Nickel (3.57 - 5.52 nM) distributions are governed by internal biogeochemical cycles, together with physical mixing and circulation patterns. Nickel is primarily removed from surface waters with biogenic particles and then remineralised at depth. Copper (1.39 - 2.89 nM) distributions illustrate a mixture of the two typical behaviours mentioned above. Distributions of typically anthropogenic and particle-reactive Pb (82 - 235 pM) are in agreement with a

Mediterranean flow source of Pb for the adjacent North Atlantic Ocean. The mechanisms controlling the biogeochemical cycling of TMs, such as atmospheric inputs, physical forcing, and interactions with primary production, are discussed according to the TM physico-chemical properties and biological importance.

Key words: Ligurian Sea; Trace metals; Seasonal variation; Mediterranean; Open water.

1. Introduction

Several trace metals (TMs), such as Fe, Co, Ni, Cu, are oceanic micronutrients that are essential to marine life (e.g., Morel and Price, 2003), while others, such as Hg or Pb, are contaminants, and evidence of the large-scale human footprint on the ocean (e.g., Hatje et al., 2018). The distributions and residence times of both TM groups in the open ocean are regulated by external inputs (aeolian deposition, riverine and submarine groundwater inputs, hydrothermal activity, pore water release) and the rates of geochemical and biologically-mediated ("biological pump") removal processes (e.g., Geibert, 2018; Lohan and Tagliabue, 2018; Wangersky, 1986). The intensity of the biological pump is, in turn, dependent on physical processes that govern primary productivity at the surface. In conjunction with the variations of TM inputs, this latter process may generate a seasonal variability of TM concentration profiles, the observations of which are sparse due to the difficulty in producing offshore TM time series (Bown et al., 2017; Connelly et al., 2006; Saito and Moffett, 2002; Tappin et al., 1993).

Here, we present the first time-series (over the duration of 18 months) of TM distribution

74 over the water column in the central Ligurian Sea, in the Western Mediterranean, that
75 allows characterisation of biogeochemical behaviours of four typical TMs (Co, Ni, Cu
76 and Pb) in an oceanic environment where the dynamics of water circulation drive a high
77 biogeochemical seasonality. Due the occurrence of strong physical forcing such as
78 horizontal and vertical advection on open waters (Béthoux, 1989), and, even more, the
79 prominent role of the atmospheric deposition (Migon et al., 2002), the Mediterranean Sea
80 is a suitable oceanic environment for studying seasonal dynamics of TMs.

81

82 **2. Site description in the Mediterranean context**

83 The Mediterranean thermohaline circulation is characterised by the inflow of Atlantic
84 water at the surface and exiting below Mediterranean Overflow Water (MOW) at
85 Gibraltar. An important consequence of this circulation is the short residence time of
86 Mediterranean waters (50 to 100 years on average; Millot and Taupier-Letage, 2005),
87 compared to that of other ocean basins (200 to 1000 years; Durrieu de Madron et al.,
88 2011). Owing to the peculiar characteristics of the basin (i.e. shallowness of the Sicily
89 Strait with 316 m maximum depth, evaporation and rain budgets, dense and bottom water
90 formation), the mean water residence time of the Western Mediterranean Sea is even
91 shorter, amounting to 22 ± 4 years (Roether et al., 2013). The process of dense water
92 formation ventilates deep waters during winter (Testor et al., 2018; Waldman et al.,
93 2018). In addition, the Western Mediterranean Sea has relatively small dimensions (e.g.,
94 the Ligurian Sea: $5.3\ 10^{10}\ m^2$), and it is subjected to significant anthropogenic pressure
95 and pulsed natural Saharan dust events (Moulin et al., 1997). In particular,atmospheric
96 deposition becomes the major source of input of TM and nutrients to the surface photic
97 layer during the stratification period (Bartoli et al., 2005; Davis and Buat-Ménard, 1990).
98 This results in significant fluxes of various elements and compounds, including trace

metals (TMs). To a large extent, the atmospheric TM inputs govern their offshore biogeochemical cycling (Guerzoni et al., 1999; Migon et al., 2002).

The DYFAMED (DYnamique des Flux Atmosphériques en MEDiterranée; Coppola et al., 2016) sampling site is located in the central zone of the Ligurian Sea, ~ 50 km off the continental French coast, 2350 m deep, 43° 25'N, 7°52' E (Fig. 1). This site is surrounded by the permanent geostrophic Ligurian frontal jet flow that results from the cyclonic circulation of the North Current, formed in the Ligurian Sea by joining the currents flowing northward along the coasts of Corsica (Millot, 1999). The North Current creates a band (~30 km width, > 250 m depth) that presumably shelters the sampling area from riverine and coastal lateral inputs by a strong horizontal density gradient (Niewiadomska et al., 2008). Acoustic Doppler Current Profiler (ADCP) measurements have shown that the DYFAMED station is isolated from the Northern Current (Andersen and Prieur, 2000), even if infrequent intrusions of waters may episodically occur in winter (Millot, 1999). As a result, the site is believed minimally affected by lateral inputs, and it is therefore commonly used as a reference site for the impact of atmospheric inputs to an oligotrophic open-ocean water column (Martín et al., 2009; Migon et al., 2002; Sarthou and Jeandel, 2001). The DYFAMED site is regarded as a one-dimensional station where simple hydrological mechanisms prevail and where the ecosystem is quite well understood (Avril, 2002). Owing to these features and its accessibility (only 50 km from Nice), the site has been chosen as a time-series observation station and has been monitored monthly since January 1991 (Marty, 2002). The site has been extensively studied for ~30 years, e.g., DYFAMED and MEDFLUX programmes; see special issues Deep-Sea Research II 49, 11 (2002) and 56, 18 (2009), respectively. The DYFAMED station is now part of the Mediterranean Ocean Observation Site for the Environment (MOOSE; http://www.moose-network.fr).

Three major water masses can be distinguished in the Ligurian Sea (Marty and Chiavérini, 2010; Millot, 1999): the surface water (0–200 m-depth), strongly affected by local climatic conditions (Schröder et al., 2006), the subjacent layer (approximately between 200 and 600 m depth at the DYFAMED site), characterised by maximum temperature and salinity due to the intrusion of Levantine Intermediate Water (LIW) (Marty and Chiavérini, 2010; Millot, 1999), and the deep layer, namely the Western Mediterranean Deep Water (WMDW), characterised by relatively low salinity and low temperature. Above all, the Ligurian Sea is subject to pronounced seasonal variations in hydrology and biology (Marty et al., 2002), with a long stratification period (May-November) during which nutrients are depleted in the photic layer. During the stratification period, atmospheric deposition becomes the major source of inputs of TMs and nutrients to the surface photic layer (Bartoli et al., 2005; Migon et al., 2002). The stratification is then disrupted in late autumn, and, in winter, due to a strong physical forcing (action of cold and dry winds, combined with low temperatures), surface waters are cooled, and their evaporation is enhanced, increasing their salinity. This process regularly initiates the formation of dense water. The subsequent vertical mixing is likely to bring amounts of nutrients from depths to surface layers, which, thus, enable early spring phytoplankton blooms (D'Ortenzio and Ribera d'Alcalà, 2009; Heimbürger et al., 2013; Migon et al., 2002). Dense water formation involves the oxygenation of deep layers. Part of this oxygen is consumed by the remineralisation of organic matter (OM) produced and settled from the photic zone.

Seasonal dynamics of phytoplankton at DYFAMED have been characterised using pigment analysis (Marty et al., 2002). The 0-200 m-depth integrated total chlorophyll a (∫TChl-a) is highly variable throughout the year and reaches the highest values during the spring bloom (up to 230 mg m^{-2}) and, evidently, the lowest values during the period of

149 the stratification period (down to 12 mg m^{-2}). Dissolved OM and TMs generally
150 accumulate within the photic layer during summer stratification and are then exported to
151 deeper layers (Avril 2002; Copin-Montégut and Avril, 1993; Heimbürger et al., 2014;
152 Migon et al., 2002).
153

154 **3. Material and Methods**

155 *3.1. Sampling*

156 In order to catch, during our sampling period, one seasonal cycle, observations over a
157 period of at least one year and a half were required (Granger, 1978). Thus, monthly
158 vertical profiles of TM and ancillary parameters were established over the duration of
159 18 months at the DYFAMED station, between June 2007 and March 2009, except in
160 December 2008 and February 2009, due to bad weather conditions. On each cruise
161 aboard the RV Téthys II, seawater was generally sampled at 12 depths from surface to
162 2200 m (150 m above the seafloor), including the main features such as the surface
163 mixed layer, TChl-a maximum, LIW, and WMDW. Hydrographic parameters were
164 obtained using a CTD profiler (Sea-bird SBE 911plus) with additional sensors
165 (dissolved oxygen and Aquatracka MKIII Chelsea fluorometer). Water samples were
166 taken using trace-clean 5-L Teflon-coated Niskin X bottles (General Oceanics 1010X)
167 fixed on a carrousel water sampler (Sea-bird SBE32) that was coated with a metal-free
168 epoxy-based paint, to allow trace-clean sampling. Prior to sampling, Niskin X bottles
169 were carefully cleaned in a clean room (Class 100) with diluted nitric acid washes
170 (Suprapur HNO_3, Merck) and deionised water rinses (Milli-Q, Millipore, resistivity 18
171 MΩ cm). Unfiltered samples were collected along the entire water column, while
172 filtered sub-samples were obtained only from the upper 50 m, where most particles and
173 phytoplankton reside (Niewadomska et al., 2008). In absence of any measurement of

174 particulate TM concentration in Mediterranean waters, we extrapolated data from other
175 places in the world ocean (Nakatsuka et al., 2007). We calculated that, at depths > 50
176 m, the particulate fraction of TMs is < 3 % and may thus be considered negligible.
177 Filtrations were performed under high-purity nitrogen pressure (1-1.2 bar), in line with
178 the Niskin bottles through filter cartridges (Sartobran 300, 0.2 µm). Sub-samples for
179 TM measurements were immediately drawn into acid-cleaned 500 mL polyethylene
180 (PE) bottles following the GEOTRACES trace-clean sample handling protocols
181 (compatible with the www.geotraces.org/images/Cookbook.pdf, version 3, 2017). They
182 were then acidified with HNO_3 (Suprapur, Merck) to pH 1. All PE bottles were
183 hermetically sealed, double-wrapped in polyethylene bags, and kept at +4°C until
184 analysis.

185 *3.2. Chemical analyses*

186 Filtered sea water samples were extracted in the clean laboratory of Centre Ifremer
187 Atlantique following Danielsson et al. (1982). Briefly, the method can be described as
188 chelation of the dissolved TMs with a mix of ammonium pyrrolidine dithiocarbamate
189 (APDC) and diethylammonium N, N-diethylcarbamate (DDDC), extraction of the
190 chelates with Freon, and back-extraction with diluted HNO_3. The obtained solutions were
191 then analysed using an inductively coupled plasma-mass spectrometer (ICP-MS, Thermo
192 Electron Corporation, Element X Series®). The detailed procedure for the extraction is
193 described elsewhere (Chiffoleau et al., 2004). Precision and accuracy were tested using
194 two Certified Reference Materials (CRM) from the National Research Council of
195 Canada, namely coastal waters (CASS-1 to 3) and open ocean water (NASS-2).
196 Precisions, calculated as the variation coefficient (i.e. confidence interval/mean) of 6
197 replicate analyses of CRMs, varied between 2 % and 9 % (Table S1, Supplementary
198 Information, SI). The detection limits were estimated 3 times the standard deviation of

199 the 6 blank replicates obtained from an analytical run. They were 8, 20, 60, and 2 pM for
200 Co, Ni, Cu, and Pb, respectively, which is low compared to the range of determined
201 concentrations (Table S2), and generally to typical oceanic concentrations (Schlitzer et al.
202 2018). Accuracies of analytical results were tested upon the results of CRM analyses;
203 they were always within the target range for certified values for the four TMs analysed.
204 Sampling quality was tested upon oceanographic consistency of the TM distributions. No
205 outliers were noticed for Co, Ni and Cu. Only a few samples, taken at the beginning of
206 the sampling period, exhibited very high Pb concentrations compared to the adjacent
207 samples. This excess decreased as the sampling programme proceeded. As they were
208 without any oceanographic consistency, we removed them from the data set (Table S2,
209 SI). Phosphate (PO_4^{3-}) and silicate ($Si(OH)_4$) concentrations were determined using a
210 standard auto-analyser according to the protocol developed by Aminot and Kérouel
211 (2007), with detection limits of 0.02 μM for both phosphate and silicate, and precisions
212 better than 6%. Pigment determination was performed using high-performance liquid
213 chromatography (HPLC) techniques described in Ras et al. (2008), ∫TChl-a being the sum
214 of chlorophyll-a + divinyl-chlorophyll-a concentrations integrated within the upper 200 m
215 of the water column. The density gradient between the surface (10 m) and the base of the
216 mixed layer (ML) estimated to determine the mixed layer depth (MLD) was 0.03 kg m^{-3}
217 (de Boyer Montégut et al., 2004; D'Ortenzio et al., 2005). For data interpretation and
218 associated statistics, we separated samples collected above 100 m depth, and samples
219 collected below 100 m depth, in order to compare TM distributions in two layers that
220 have contrasted concentration profiles. This approach is justified because the MLD never
221 extended beyond 100 m during the present sampling period (Pasqueron de Fommervault
222 et al., 2015).
223 *3.3. Statistical analysis*

Parametric (Student t-test, Pearson correlation) and non-parametric (Wilcoxon, Mann-Whitney) statistical tests were applied to variables after testing for the normality of distributions (Shapiro-Wilk and Fisher tests). The statistical computations were performed with XLSTAT software from Addinsoft (https://www.xlstat.com/). The frequency distributions of TM concentrations showed some departure from normal-distributions (Fig. S1 and Table S3, SI). Thus, in order to describe central tendency measurements, we calculated geometric means and median, in addition to arithmetic means and standard deviations (Table 1).

4. Results and Discussion

4.1. Hydrological and biological seasonal patterns

Salinity varied between 38.02 and 38.62, within the range usually found at this station (Marty et al., 2002). Vertical salinity profiles always followed the well-known pattern for this site, with lowest values in the ML, maximum values between 200 and 600 m (LIW) and moderate values below 600 m (WMDW). Temperature ranged from 12.9 to 24.6°C, with highest values in the shallow ML (~10 m) at the end of summer. Vertical temperature profiles converged below 1000 m-depth to approximately 12.9°C, while the overlying LIW was slightly warmer with approximately 13.4°C. Seasonal patterns of MLD during the sampling period are shown in Fig. 2 (see also Pasqueron de Fommervault et al., 2015). The water column remained well stratified most of the time, and only slight winter mixing occurred. In contrast to usual MLD values of 100 - 200 m (Heimbürger et al., 2013; Marty et al., 2002) or more (> 2000 m-depth in 2006; Marty and Chiavérini, 2010) during winter mixing, the MLD never exceeded 70 m-depth during our sampling period (Fig. 2). Among other physical forcing factors, MLD is viewed to have the strongest impact on phytoplankton dynamics (Lavigne et al., 2013).

249 The relatively shallow MLD observed during our sampling period may not be deep
250 enough to supply sufficient macronutrients and, therefore, may be responsible for the low
251 primary productivity resulting in low values of ∫TChl-a. However, TChl-a varied
252 intensely over the sampling period (Fig. 2); its distribution reveals spring and autumn
253 phytoplankton blooms within the upper 50 m (Fig. 2). Values of ∫TChl-a were in the
254 range of those usually found (12 - 230 mg m^{-2}) at this site (Marty et al., 2002), ranging
255 between 16 and 170 mg m^{-2}.

256 An outstanding feature is the high ∫TChl-a value in October 2007 (77 mg m^{-2}). Nutrients
257 from subsurface layers were likely raised to the surface layer by the permanent cyclonic
258 circulation of the area (D'Ortenzio et al., 2014). Due to the relative shallowness of
259 nutriclines in this region, wind events can inject some nutrients to the depleted surface
260 layer, hence an increase of chlorophyll concentration. Furthermore, exceptionally high
261 ∫TChl-a values were associated to the period when winter convection takes usually place
262 (January-February 2008, 102 and 123 mg m^{-2}, respectively; Fig. 2), in spite of a very
263 shallow MLD measured in winter 2008 (Coppola et al., 2018). Before the use of
264 autonomous platforms capable of acquiring high-frequency data (i.e. the time of our
265 sampling), MLD measurements were made during monthly on-site campaigns scheduled
266 a year in advance, involving recurring uncertainty in the measurement of a process of
267 relatively short duration. Hence the possibility of incorrect estimates of the MLD, likely
268 to yield errors in the concentration of nutrients brought to surface waters by the winter
269 convection process. Such incorrectly estimated (underestimated) MLD can lead to a
270 mismatch between the calculated nutrient supply, the amount of Chl-a that can be
271 sustained by such a supply, and the actual observed Chl-a concentration. After the spring
272 bloom in April 2008 (∫TChl-a = 170 mg m^{-2}), ∫TChl-a remained greater than 40 mg m^{-2}
273 until September 2008.

Figures 3a and b present the vertical PO_4^{3-} and $Si(OH)_4$ concentration distributions, respectively, over the entire water column for the whole sampling period. The general shape of these profiles was typical of the distribution usually observed at the DYFAMED site (Marty et al., 2002), with highest concentrations between 500 and 1000 m-depth, especially between March and July 2008, and lowest concentrations in the surface layer. Deepening of the ML, in March 2008 and January 2009, down to 41 and 69 m, respectively (Fig. 2), lead to partial homogenisation, after which slightly higher macronutrient concentrations were present in the ML, in March 2008 and 2009, that is 0.08 to 0.15 µM for PO_4^{3-} and 1.4 to 3.7 µM for $Si(OH)_4$ (Fig. 3).

In summary, our sampling period from mid-2007 to mid-2009 displayed (i) a highly stratified water column with only little dense water formation in winter (based on MLD values measured at DYFAMED), and (ii) phytoplankton blooms in spring and late summer-early autumn (especially autumn 2007).

4.2. Trace metal distributions

The most striking characteristic of the TM distribution in the Ligurian Sea over the 18-month sampling period is the high concentration of Pb. On the contrary, when comparing the present data with those of the Schlitzer, eGEOTRACES – Electronic Atlas (Geotraces Electronic Atlas, 2019), it appears that Co, Cu and Ni concentrations were within the ranges usually found in open oceanic waters of the Mediterranean Sea (Schlitzer et al. 2018). Historical literature data are recorded in Table S4 (SI) for comparison. While most TMs changed little over time, Pb concentration decreased continuously during the last 20 years (see discussion below). Major variations of the present TM time series occurred in the upper 100 m (Fig. 4), where physical, chemical and biological forcing is the most intense. Below 100 m, most TM concentration profiles converged rapidly toward a relative uniformity, indicating a rapid mixing time

or a common export mechanism with little temporal variability. Basic processes occurring in the water column can be assessed by running a simple vertical two-box model, separating the euphotic layer (< 100 m) from the deep reservoir (> 100 m) at DYFAMED. The four TMs studied have significantly different mean concentrations ($p < 0.01$) between the euphotic (< 100m) and deeper waters (> 100m) (see statistical tests in Table 1). On the one hand, mean concentrations were higher in the deep waters than in the euphotic layer for Ni and Cu, confirming their "nutrient-like" behaviour. On the other hand, mean concentrations were higher in the euphotic layer than in deep waters for Co and Pb, which confirms the "surface-enriched/scavenging" type of their vertical distribution, underlining the importance of atmospheric sources for these two TMs. We did not observe any increase in TM concentrations near the bottom that suggests negligible benthic TM source. This idea needs further consideration since our sampling did not include the bottom 150 m of the water column. This water layer may contain deep-sediment resuspension resulting from bottom-reaching winter convection, or deep cascading events occurring in Western Mediterranean Sea (Durrieu de Madron et al., 2017). Generally, there is no nepheloid bottom layer at DYFAMED, except for rare cases of very strong events of deep convection and cascading, e.g., in 1999 (Béthoux et al., 2002), or, even more, in 2006, when an exceptional episode of deep convection occurred (Martín et al., 2010). As already mentioned, the process of dense water formation was not very significant during the sampling period considered here, and the presence of a nepheloid layer is unlikely.

Cobalt concentrations varied from 22 to 172 pM, and were high in the upper 100 m (up to 172 pM at surface; Table 1) and decreased rapidly within the upper 200 m to fairly uniform concentrations of 41 ± 8 pM, a value very close to the 45 pM determined in the WMDW (Dulaquais et al., 2017). Such a distribution is typical of surface-

enriched/scavenged-type behaviour of TMs having a large atmospheric source. The winter surface concentrations are as high or higher than those measured in summer, i.e. around 100 pM (Fig. 4a). This might be due, in 2008, to the relatively late occurrence of the convection process (Coppola et al., 2018), i.e. in March. At the end of the spring bloom, dissolved Co concentration is minimal because of its consumption by plankton. As oligotrophy increases, Co consumption decreases and, at the same time, atmospheric deposition refuels surface waters. Thus, the stock of dissolved Co increases to presumably reach its maximum level before the convective export. In 2009, no significant mixing was observed at DYFAMED (Coppola et al., 2018). Consequently, our results did not show any pronounced seasonal difference in the general distribution pattern. Vertical Co profiles always conserved their surface-enriched shape, as observed in the entire Mediterranean Sea (Dulaquais et al., 2017). However, some seasonal pattern in the surface layer can be recognised. High Co surface concentrations (> 100 pM) were observed from October 2007 to March 2008, suggesting that above-average atmospheric loads of Co were deposited to surface waters and have lead to the accumulation of dissolved Co between the end of the plankton bloom and the dense water formation episode, i.e. an oligotrophic period during which there is almost no export, due to the absence of biological activity to allow vertical transfer (e.g., Migon et al., 2002; Passow, 2004; Heimbürger et al., 2014). This ended when the process of dense water formation took place, allowing a rapid export of dissolved matter. As well, Co concentrations in the surface layer peaked up to 164 - 172 pM in January 2009 (Fig. 4a). Indeed, although no data on atmospheric deposition were available in 2009, very high Co concentrations were measured in the atmospheric aerosol (Cap Ferrat sampling station) in October 2008 (up to 11 $\mu mol\ m^{-3}$ while the mean aerosol Co concentration was $1.8 \pm 1.3\ \mu mol\ m^{-3}$ between January 2006 and December 2008; Heimbürger et al., 2010). Estimations of seawater-

labile Co inputs to the surface of the Ligurian Sea ranged between 0.08 - 6 μmol m^{-2} d^{-1} (Heimbürger et al., 2011). The increase of concentrations in the atmospheric aerosol observed in October 2008 suggests an increase of Co deposition fluxes as well. This atmospheric input occurred during the oligotrophic period, and its seawater-labile fraction was presumably transferred to depth only during the formation of dense water. Furthermore, the statistically significant negative correlation between Co and salinity ([Co](pM) = –187[Salinity](psu) + 7242, n = 204, R = 0.80 for a salinity range comprised between 38.0 and 38.6 psu) suggests that the atmospheric Co source consists mainly of wet deposition, the influence of riverine discharge being very low in the Ligurian Sea, overall.

Lower concentrations (< 100 pM) were observed from April to September 2008, in agreement with uptake by phytoplankton in spring. Cobalt is a bioactive TM of considerable importance in biogeochemical processes occurring in the global ocean (Morel, 2008), but also the scarcest of all known bioactive TMs (Saito et al., 2017). Owing to its surface-enriched pattern, the steep decrease of Co within the upper 200 m-depth should not be related to its consumption by PP, but may be attributed, at least partially, to adsorption onto sinking particles (Fisher et al., 1991) and further transfer to the marine sediment. In oligotrophic waters, the bioactive character of Co may be crucial, but it is very likely outweighed by the relative importance of atmospheric inputs in the Northwestern Mediterranean (Guerzoni et al., 1999; Marín et al., 2017). In spite of this important bioactive role, Co surface depletions are not usually seen unless Zn values are low, according to the hypothesis that Co may replace Zn in marine phytoplankton, when Zn becomes depleted (Morel, 2008; Sunda and Huntsman, 1995). Considering the relatively high values of Co and Zn in Northwestern Mediterranean waters (Migon, 2005), the occurrence of this substitution mechanism remains unlikely. When PP was

maximal (February-April 2008, March 2009), surface-enriched Co profiles were always conserved (Fig. 4a).

Cobalt is strongly bound by ligands, and the speciation study of Saito and Moffett (2001) suggests that a fraction of Co might not be detectable by many analytical methods without UV-oxidation procedure. This possible bias, not detectable by the analysis of CRM samples, might affect Co concentrations, but presumably not Co biogeochemical behaviour, as Co exhibits relatively high concentrations in surface, compared with oceanic regions, and its distribution is characterised by accumulation in surface waters. We infer that the distribution of Co in the upper water column is mainly controlled by steady inputs of atmospheric crustal material, while biological activity, even in mesotrophic conditions (spring bloom), is not capable of removing Co from surface waters to the point of surface depletion. In summary, the present data set suggests that Co does not co-limit PP in the Northwestern Mediterranean basin, because of high atmospheric inputs. Future increased large-scale use of Co for automotive batteries will likely further increase Co inputs to the Mediterranean Sea, and the Global Ocean as well (Zhang et al., 2016).

Nickel concentrations varied from 3.57 to 5.52 nM, with a mean of 4.54 ± 0.39 nM (Table 1). These concentrations are comparable to those previously published for the western Mediterranean (Table S4, SI, according to Morley et al., 1997 and Yoon et al., 1999), and vary only little with time and depth (Fig. 4b). The variability of the observed seawater values (8.6%) approaches the analytical precision (5%). However, the graphical illustration of the profile series suggests lower concentrations in the euphotic waters (Fig. 4b), which is attested by statistical tests ($p < 0.01$, Table 1). High PP in spring (2008 and 2009) lead to the lowest Ni surface concentrations (Fig. S3). Nickel displayed typical nutrient-like profiles throughout the sampling period. The low surface concentrations are

399 explained by biological uptake (Dupont et al., 2007), while higher deep-water
400 concentrations are presumably due to the export flux of OM with a subsequent release
401 during remineralisation. Indeed, Ni is significantly correlated ($p < 0.01$) with phosphate
402 ([Ni](nM) = 1.80 [PO_4^{3-}](μM) + 4.03, n = 180, R = 0.81), and silicate ([Ni](nM) = 0.09
403 [$Si(OH)_4$](μM) + 4.03, n = 169, R = 0.77), as previously pointed out by, e.g., Achterberg
404 et al. (1993). The lowest surface Ni concentrations are presumably due to the
405 consumption of the Ni stock during the spring bloom. In addition, it is likely that the
406 uptake by PP is not balanced by atmospheric inputs, which are usually low in winter
407 (Heimbürger et al., 2010). In all cases, Ni profiles were fairly uniform at depth, with no
408 noticeable change in the different seasons, as already stated by Morley et al. (1997). In
409 summary, the present data indicate that Ni distributions are largely controlled through
410 uptake by microorganisms and remineralisation from settling particles, as already
411 suggested by Cid et al. (2011).

412 **Copper** concentrations varied between 1.39 and 2.89 nM with a mean of 1.99 ± 0.28 nM
413 (Table 1 and Fig. 4c). Values in the same range have been observed since the 1980s
414 (Table S3, SI, according to Béthoux et al., 1990; Boyle et al., 1985; Morley et al., 1997).
415 Although, on a yearly basis, Cu concentration were lower in the euphotic layer than
416 deeper ($p < 0.01$, Table 1), surface-enriched Cu profiles (e.g., December 2007) alternated
417 with surface-depleted ones (e.g., May 2008), and uniform profiles also occurred (e.g.,
418 March 2009). Surface depletion occurred when driving forces of vertical export
419 (hydrology with dense water formation, or biology in productive conditions; Migon et al.,
420 2002) were active, while surface accumulation occurred under summer/autumn
421 conditions of oligotrophy with little uptake by PP. This scheme was not always clear,
422 however. For example, in 2008, Cu vertical distributions shifted from surface-depleted
423 profile (February) to surface-enriched profile (March), and then shifted again toward

surface-depleted profiles (April and May; Fig. 4c). Such a scenario may seem surprising, because the maximum deepening of the ML in 2008 was observed in March (Fig. 2), which suggests a hydrologically-driven transfer of matter to depth, thus no accumulation in surface. As Cu concentrations in the atmospheric aerosol were regularly decreasing between February and May 2008 (Heimbürger et al., 2010) the possibility of atmospheric loads capable of counterbalancing this transfer is unlikely. Therefore, we think the most plausible explanation is the inaccuracy of field data on the exact time of winter convection process as already pointed out by Heimbürger et al. (2013). More generally, Cu, in spite of its well-known biological role, rarely depicted nutrient-like profiles in the Northwestern Mediterranean, as observed in the global ocean, e.g., Pacific (Bruland, 1980; Nozaki, 1997). In the oligotrophic waters of the Northwestern Mediterranean, the bioactive character of Cu is probably outweighed by the relative importance of atmospheric inputs. However, biological uptake during spring bloom seems capable of consuming important Cu quantities, inducing a rapid shift toward surface-depleted profiles as observed as soon as in April 2008 (Fig. 4c). This strong dependence of Cu dynamics on biological activity (seasonality) highlights the importance of temporal observations. In particular for Cu, one has to take into account the current state of PP in the interpretation of a vertical Cu profile. For example, Boyle et al. (1985) and Seyler et al. (1989) found nutrient-like profiles for Cu just after the spring bloom. On the contrary, others reported a more or less homogeneous distribution, with, perhaps, a slight surface-enrichment (Béthoux et al., 1990; Ferrara and Seritti, 1989; Yoon et al., 1999). In summary, Cu profiles in surface waters seem close to the rectilinearity, presumably resulting from equilibrium between removal by plankton consumption and atmospherically-deposited loads. This would result in a shift between surface-depleted Cu profiles in periods of high biological activity and surface-enriched Cu in periods of

449 oligotrophy.

450 **Lead** concentrations ranged from 82 (below 100 m-depth) to 235 pM (above 100 m-
451 depth) with a mean value of 117 ± 24 pM over the 0-2200 m-depth water column (Table
452 1). Lead concentrations depicted intense variation in the euphotic layer (Fig. 4d), but
453 minor, although statistically significant, enrichment compared to the deep waters (Table
454 1), with a large variability of the concentrations in the water column (24%). Basically, Pb
455 concentrations exhibit surface-enriched profiles. Compared to previous published data,
456 Pb concentrations in the Western Mediterranean Sea have decreased over time in surface
457 waters (0-100m, approximately) (Nicolas et al., 1994; Migon and Nicolas, 1998; Table
458 S4, SI). Moreover, we found surface Pb concentrations similar to those found earlier in
459 deep waters. This results from the decrease of external fluxes since mid-1980s, mainly
460 atmospheric deposition (Migon et al., 1993; Migon et al., 2008). While atmospheric Pb
461 concentrations in the Mediterranean troposphere decreased by 90% between 1987 and
462 2008 (Heimbürger et al., 2010), a smaller decrease was observed in seawater Pb
463 concentrations. The Pb concentrations of the upper 100 m decreased by 60%, from 300-
464 362 pM (Seyler et al., 1989; Marty and Nicolas, 1993) to 126 pM, and by 20% in waters
465 below 100 m depth, from 130-145 pM (Seyler et al., 1989; Marty and Nicolas, 1993) to
466 108 pM respectively).

467 Using the mean concentration of deep Pb (108 pM, Table 1) as the typical Pb
468 concentration in the MOW, this concentration is more than twice the concentration found
469 in the North Atlantic at the same depth (< 40 pM according to Boyle et al., 2014).
470 Moreover, this is consistent with the recent results by Zurbrick et al. (2018), who found
471 that Pb concentrations in the Atlantic off the Portugal coasts were the highest in
472 subsurface Mediterranean waters, i.e., ~ 60 pM in the core of the MOW body. Likewise,
473 increased dissolved Pb concentrations observed along GEOTRACES transects in the

Northeastern Atlantic were identified as MOW inputs (Rolison, 2016). Rusiecka et al. (2018) have described the spreading of MOW across Northeast Atlantic at intermediate depth.

4.3. Trace metal behaviours: sorting physical and biogeochemical processes

In summary, one can find at a single offshore site (DYFAMED), on a temporal scale, all the behaviours previously observed on a geographic scale. The four TMs (Ni, Cu, Co and Pb) exhibit a range of biogeochemical behaviours that can be characterised by two typical concentration profiles, surface-depleted (nutrient-like) and surface-enriched (scavenged-type). Nutrient-like metals, best exemplified here by Ni, are primarily removed from surface waters by biogenic particles and then remineralised at depth. Internal biogeochemical cycles, together with physical mixing and circulation patterns, control the distributions of nutrient-like TMs. Scavenged-type metals, exemplified here by Co and Pb, are scavenged by particulate matter and continue to be removed onto particles in intermediate and deep waters as well as at the surface. External inputs, such as the deposition of aeolian dust, largely control the concentrations and distributions of scavenged-type TMs, which result from the equilibrium between atmospheric supply and removal by scavenging and sometimes uptake (e.g., Co). Overall, this equilibrium results in a surface enrichment, the magnitude of which varies over the season as the supply and removal respective intensities vary. Surface Cu distribution results from the balance between atmospheric supply and biological uptake. When supply outcompetes uptake, Cu accumulates in the surface layer. For Ni, the supply never leads to surface accumulation, but these two bioactive TMs both behave like nutrients rather than scavenged-type TMs, because deep concentrations of both are not depleted, which is the identifying feature of nutrient-like elements.

In the Mediterranean area, TMs with significant crustal/natural sources (Co, Ni, and, to a

lesser extent, Cu) are characterised by higher atmospheric inputs during summer, owing to pulsed Saharan dust emissions (Marticorena and Bergametti, 1996). On the contrary, atmospheric fluxes of anthropogenic TMs such as Pb are generally higher in winter (Duncan and Bey, 2004; Heimbürger et al., 2010; Migon et al., 2008). However, we could not observe any evident coupling of TM vertical distributions with seasonal variation of atmospheric TM inputs measured during the same period on the nearby coastal sampling site Cap Ferrat (Heimbürger et al., 2010). This might support the hypothesis that atmospheric deposition does not determine marine vertical export flux of metals, but accumulates in the marine surface layer, awaiting to be exported by hydrological or biological means (Heimbürger et al., 2014; Migon et al., 2002). Particle-reactive TMs are rapidly removed from the water column to the marine sediment. For example, Pb adsorbs onto particles (e.g., Bridgestock et al., 2018; Shen and Boyle, 1988) and co-precipitates on iron/manganese oxides (Tanguy et al., 2011; Waeles et al., 2007), hence its scavenging-type behaviour. Removal processes of such TMs are mainly governed by biological activity and their residence times (e.g., Cu and Pb, ~9 and 0.5 years; Nicolas et al., 1998) are generally lower than the WMDW residence time. Due to the rapid ventilation of Mediterranean waters, Pb concentrations evolved rapidly, almost concomitantly with atmospheric changes (Migon and Nicolas, 1998; Heimbürger et al., 2010). The signature of this evolution has been found in the MOW, which feed into the Atlantic Ocean (Noble et al., 2015; Zurbrick et al., 2018). However, Pb concentrations remain higher than in other oceanic environments of the northern hemisphere, suggesting the persistence of the anthropogenic emissions.

In summary, the 18-month time series presented in this paper allowed to exemplify the superimposed effects of water stratification, atmospheric input and biological pump on the vertical distribution of TMs in a particular open-sea system. The short residence

time of waters, the alternation of deep convection and water stratification, and the succession of different trophic states of the Ligurian Sea, make it a suitable environment to illustrate the entanglement of these processes. The present study allows to sort out the influence of biogeochemical and physical parameters on TM distribution in the water column of a low-nutrient low-chlorophyll region, the Ligurian Sea (Western Mediterranean). The Ligurian Sea is an epicontinental sea where deep waters are formed during winter convection. Our results showed that Co, Cu and Ni concentrations were within the ranges found in other open oceanic waters and were not limiting the primary production, whereas Pb levels characterised anthropogenic inputs, albeit its 20% concentration decrease recorded in deep waters in the last 20 years. Winter convection spreads Pb contamination in the deep waters of the entire Western Mediterranean, suggesting that the Mediterranean outflow is the source of Pb contamination, observed at around 1000 m depth, in the adjacent Eastern North Atlantic Ocean.

Acknowledgements

This research was supported by the Ifremer project MEDICIS (Mediterranean Contaminants Identification System) and the PACA Region, with the participation of the Agence de l'Eau Rhône-Méditerranée-Corse. We would like to thank the captain and the crew of the RV TETHYS II, Céline Bachelier, Gaël Durrieu, Grigor Obolensky and Vincenzo Vellucci for their work at sea. We thank Emmanuelle Rozuel and Dominique Auger for their work in the clean-laboratory of Centre Ifremer Atlantique. We are also grateful to the BOUSSOLE project, Laurent Coppola (Service d'Observation du Laboratoire d'Océanographie de Villefranche), Francis Louis and Roger Kérouel (Centre

549 Ifremer de Bretagne).

550

551 **References**

552 Achterberg, E.P., Zhang, H., Gledhill, M., Van den Berg, C.M.G., 1993. Chemical
553 speciation of chromium and nickel and the concentration of iron and platinum in the
554 western Mediterranean. Wat. Pollut. Res. Reports 30, 163-169.

555 Aminot, A., Kérouel, R., 2007. Dosage automatique des nutriments dans les eaux
556 marines : méthodes en flux continu. MEDD and Quae Publishers, France, 188pp, ISBN:
557 10 275920023X.

558 Andersen, V., Prieur, L., 2000. One-month study in the open NW Mediterranean Sea
559 (DYNAPROC experiment, May1995): overview of the hydrobiogeochemical structures
560 and effects of wind events. Deep-Sea Res. I 47, 397-422, doi:10.1016/S0967-
561 0637(99)00096-5.

562 Avril, B., 2002. DOC dynamics in the northwestern Mediterranean Sea (DYFAMED
563 site). Deep-Sea Res. II 49, 2163-2182, doi:10.1016/S0967-0645(02)00033-4.

564 Bartoli, G., Migon, C., Losno, R., 2005. Atmospheric input of dissolved inorganic
565 phosphorus and silicon to the coastal northwestern Mediterranean Sea: fluxes,
566 variability and possible impact on phytoplankton dynamics. Deep-Sea Res. I 52, 2005–
567 2016, doi.org/10.1016/j.dsr.2005.06.006.

568 Béthoux, J.P., 1989. Oxygen consumption, new production, vertical advection and
569 environmental evolution of the Mediterranean Sea. Deep-Sea Res. I 36, 5, 769-781,
570 doi:10.1016/0198-0149(89)90150-7.

571 Béthoux, J.P., Courau, P., Nicolas, E., Ruiz-Pino, D., 1990. Trace metal pollution in the
572 Mediterranean Sea. Oceanol. Acta 13, 481-488.

573 Béthoux, J.P., Durrieu de Madron, X., Nyffeler, F., Tailliez, D., 2002. Deep water in the
574 western Mediterranean: peciuliar 1999 and 2000 characteristics, shelf formation
575 hypothesis, variability since 1970 and geochemical inferences. J. Mar. Syst. 33-34, 117-
576 131, doi:10.1016/S0924-7963(02)00055-6.

577 Boyle, E.A., Chapnick, S.D., Bai, X.X., Spivack, A., 1985. Trace metal enrichments in
578 the Mediterranean Sea. Earth Planet. Sci. Lett. 74, 405-419, doi:10.1016/S0012-
579 821X(85)80011-X.

580 Boyle, E.A., Lee, J.M., Echegoyen, Y., Noble, A., Moos, S., Carrasco, G., Zhao, N.,
581 Kayser, R., Zhang, J., Gamo, T., Obata, H., Norisuye, K., 2014. Anthropogenic lead
582 emissions in the ocean: The evolving global experiment. Oceanography 27, 69–75,
583 doi:10.5670/oceanog.2014.10.

584 Bown, J., Laan, P. Ossebaar, S., Bakker, K., Rozema, P., de Bar, H.J.W., 2017.
585 Bioactive trace metal time series during Austral summer in Ryder Bay, Western
586 Antarctic Peninsula. Deep-Sea Res. II, 139, 103-119.

587 Bridgestock, L., Rehkamper, M., van de Flierdt, T., Paul, M., Milne, A., Lohan, M.C.,
588 Achterberg, E.P., 2018. The distribution of lead concentrations and isotope
589 compositions in the eastern Tropical Atlantic Ocean. Geochem. Cosmochim. Acta 225,
590 36-51.

591 Bruland, K.W., 1980. Oceanographic distributions of cadmium, zinc, nickel, and copper
592 in the North Pacific. Earth Planet. Sci. Lett. 47, 176-198, doi:10.1016/0012-
593 821X(80)90035-7.

594 Chiffoleau, J.F., Auger, D., Chartier, E., 2004. Dosage de certains métaux-traces (Cd,
595 Co, Cu, Fe, Ni, Pb, Zn) dissous dans l'eau de mer après extraction liquide-liquide.
596 Programme scientifique Seine-Aval, Plouzané, France, 40pp, ISBN: 2-84433-104-1.

Cid, A.P., Urushihara, S., Minami, T., Norisuye, K., Sohrin, Y., 2011. Stoichiometry among bioactive trace metals in seawater on the Bering Sea shelf. J. Oceanogr. 67, 3, 747-764, doi:10.1007/s10872-011-0070-z.

Connelly, D.A., Statham, P.J., Knap, A.H., 2006. Seasonal changes in speciation of dissolved chromium in the surface Sargasso Sea. Deep-Sea Res. I 53, 1975-1988.

Copin-Montégut, G., Avril, B., 1993. Vertical distribution and temporal variation of dissolved organic carbon in the North-Western Mediterranean Sea. Deep-Sea Res. I 40, 1963-1972, doi:10.1016/0967-0637(93)90041-Z.

Coppola, L., Diamond Riquier, E., Carval J.Y., 2016. DYFAMED observatory data. SEANOE, doi.org/10.17882/43749.

Coppola, L., Legendre, L., Lefevre, D., Prieur, L., Taillandier, V., Diamond-Riquier, E., 2018. Seasonal and inter-annual variations of dissolved oxygen in the northwestern Mediterranean Sea (DYFAMED site). Progr. Oceanogr. 162, 187-201, doi:10.1016/j.pocean.2018.03.001.

Danielsson, L.G., Magnusson, B., Westerlund, S., Zhang, K., 1982. Trace metal determinations in estuarine waters by electrothermal atomic absorption spectrometry after extraction of dithiocarbamate complexes into Freon. Anal. Chim. Acta 144, 183-188, doi:10.1016/S0003-2670(01)95531-X.

de Boyer Montégut, C., Madec, G., Fischer, A.S., Lazar, A., Iudicone, D., 2004. Mixed layer depth over the global ocean: An examination of profile data and a profile-based climatology. J. Geophys. Res. 109, C12003, doi:10.1029/2004JC002378.

D'Ortenzio, F., Iudicone, D., de Boyer Montégut, C., Testor, P., Antoine, D., Marullo, S., Santoleri, R., Madec, G., 2005. Seasonal variability of the mixed layer depth in the Mediterranean Sea as derived from in situ profiles. Geophys. Res. Lett. 32, L12605,

621 doi:10.1029/2005GL022463.

622 D'Ortenzio, F., Lavigne, H., Besson, F., Claustre, H., Coppola, L., Garcia, N., Laës-
623 Huon, A., Le Reste, S., Malardé, D., Migon, C., Morin, P., Mortier, L., Poteau, A.,
624 Prieur, L., Raimbault, P., Testor, P., 2014. Observing mixed layer depth, nitrate and
625 chlorophyll concentrations in the North Western Mediterranean: a combined satellite
626 and NO_3 profiling floats experiment. Geophys. Res. Lett. 41, 6443-6451,
627 doi:10.1002/2014GL061020.

628 D'Ortenzio, F., Ribera d'Alcalà M., 2009. On the trophic regimes of the Mediterranean
629 Sea: a satellite analysis. Biogeosciences 6, 2, 139–148, doi:10.5194/bg-6-139-2009.

630 Dulaquais, G., Planquette, H., L'Helguen, S., Rijkenberg, M.J.A., Boyé, M., 2017. The
631 biogeochemistry of cobalt in the Mediterranean Sea. Global Biogeochem. Cycles 31, 2,
632 377-399, doi:10.1002/2016GB0054780.

633 Duncan, B.N., Bey, I., 2004. A modelling study of the export pathways of pollution
634 from Europe: seasonal and interannual variations (1987–1997). J. Geophys. Res.
635 Atmos. 109, D08301, doi:10.1029/2003JD004079.

636 Dupont C.L., Barbeau, K., Palenik, B., 2007. Ni uptake and limitation in marine
637 Synechococcus. Appl. Environ. Microbiol. 74, 1, 23-31, doi:10.1128/aem.01007-07.

638 Ferrara, R., Seritti, A., 1989. Mercury and trace metals in waters of the Western
639 Mediterranean. Wat. Pollut. Res. Reports 13, 199-206.

640 Durrieu de Madron, X. et al., 2011. Marine ecosystems' responses to climatic and
641 anthropogenic forcings in the Mediterranean. Progr. Oceanogr. 91, 97-166,
642 doi:10.1016/j.pocean.2011.02.003.

643 Durrieu de Madron, X., Ramondenc, S., Berline, L., Houpert, L., Bosse, A., Martini, S.,
644 Guidi, L., Conan, P., Curtil, C., Delsaut, N., Kunesch, S., Ghiglione, J.F., Marsaleix, P.,

645 Pujo-Pay, M., Séverin, T., Testor, P., Tamburini, C., and the ANTARES collaboration.
646 Deep sediment resuspension and thick nepheloid layer generation by open-ocean
647 convection. J. Geophys. Res. Oceans 122, 2291-2318, doi:10.1002/2016JC012062.
648 Fisher, N.S., Nolan, C.V., Fowler, S.W., 1991. Scavenging and retention of metals by
649 zooplankton fecal pellets and marine snow. Deep-Sea Res. I 38, 10, 1261–1275,
650 doi:10.1016/0198-0149(91)90026-C.
651 Frache, R., Baffi, F., Dadone, A., Zanicchi, G., 1976. The determination of heavy
652 metals in the Ligurian Sea. I, the distribution of Cu, Co, and Cd in surface waters. Mar.
653 Chem. 4, 365-375, doi:10.1016/0304-4203(76)90021-9.
654 Geotraces Electronic Atlas, 2019. *Schlitzer, eGEOTRACES – Electronic Atlas of*
655 *GEOTRACES Sections and Animated 3D Scenes, http://www.egeotraces.org, 2019.*
656 Granger, C.W.J., 1978. Seasonality, Causation, Interpretation, and Implications:
657 Seasonal Analysis and Economy Time Series, Arnold Zellner Ed., U.S. Bureau of the
658 Census, pp. 33-55.
659 Guerzoni, S., Chester, R., Dulac, F., Moulin, C., Herut, B., Loÿe-Pilot, M.D., Measures,
660 C., Migon, C., Molinaroli, E., Rossini, P., Saydam, C., Soudine, A., Ziveri, P., 1999.
661 The role of atmospheric deposition in the biogeochemistry of the Mediterranean Sea.
662 Progr. Oceanogr. 44, 1-3, 147-190, doi:10.1016/S0079-6611(99)00024-5.
663 Hatje, V., Lamborg, C.H., Boyle, E.A., 2018. Trace-Metal Contaminants: Human
664 Footprint on the Ocean. Elements 14, 403-408.
665 Heimbürger, L.E., Lavigne, H., Migon, C., Coppola, L., D'Ortenzio, F., Estournel, C.,
666 Miquel, J.C., 2013. Interannual variability of 200m-depth mass fluxes at the
667 DYFAMED time-series station (Ligurian Sea). Progr. Oceanogr. 119, 59-67,
668 doi:10.1016/j.pocean.2013.08.005.

669 Heimbürger, L.E., Migon, C., Dufour, A., Chiffoleau, J.F., Cossa, D., 2010. Decadal
670 trends and evolutions of trace-metals (Al, Cd, Co, Cu, Fe, Mn, Ni, Pb, Zn) in the
671 western Mediterranean atmosphere. Sci. Total Environ. 408, 2629-2638,
672 doi:10.1016/j.scitotenv.2010.02.042.

673 Heimbürger, L.E., Migon, C., Losno, R., Miquel, J.C., Thibodeau, B., Stabholz, M.,
674 Dufour, A., Leblond, N., 2014. Vertical export flux of metals in the Mediterranean Sea.
675 Deep-Sea Res. I 87, 14-23, doi:10.1016/j.dsr.2014.02.001.

676 Jackson, J.E., 2003. A User's Guide to Principal Components. Wiley Series in
677 Probability and Statistics, J. Wiley and Sons, 592 pp.

678 Lavigne, H., D'Ortenzio, F., Migon, C., Claustre, H., Testor, P., Ribera d'Alcalà, M.,
679 Lavezza, R., Houpert, L., Prieur, L., 2013. Enhancing the comprehension of mixed
680 layer depth control on the Mediterranean phytoplankton phenology. J. Geophys. Res.
681 Oceans 118, 3416-3430, doi:10.1002/jgrc.20251.

682 Lévy, M., Mémery, L., André, J.M., 1998. Simulation of primary production and export
683 fluxes in the Northwestern Mediterranean Sea. J. Mar. Res. 56, 197-238,
684 doi:10.1357/002224098321836163.

685 Lohan, M.C., Tagliague, A., 2018. Oceanic Micronutrients: Trace Metals that are
686 essential for Marine Life. Elements, 14: 385-390.

687 Marticorena, B., Bergametti, G., 1996. Two-year simulations of seasonal and
688 interannual changes of the Saharan dust emissions. Geophys. Res. Lett. 23, 1921–4,
689 doi:10.1029/96GL01432.

690 Marín, I., Nunes, S., Sánchez-Pérez, E.D., Aparicio, F.L., Estrada, M., Marrasé, C.,
691 Moreno, T., Wagener, T., Querol, X., Peters, F., 2017. Anthropogenic versus mineral
692 aerosols in the simulation of microbial planktonic communities in coastal waters of the

693 northwestern Mediterranean Sea. Sci. Total Environ. 574, 553-568,
694 doi:10.1016/j.scitotenv.2016.09.005.

695 Martín, J., Miquel, J.C., Khripounoff, A., 2010. Impact of open sea deep convection on
696 sediment remobilization in the western Mediterranean. Geophys. Res. Lett. 37, L13604,
697 doi:10.1029/2010GL043704.

698 Martín, J., Sanchez-Cabeza, J.A., Eriksson, M., Levy, I., Miquel, J.C., 2009. Recent
699 accumulation of trace metals in sediments at the DYFAMED site (Northwestern
700 Mediterranean Sea). Mar. Pollut. Bull. 59 (4–7), 146–153,
701 doi:10.1016/j.marpolbul.2009.03.013.

702 Marty, J.C., 2002. The DYFAMED time-series program (French-JGOFS). Deep-Sea
703 Res. II 49, 1963-1964, doi:10.1016/S0967-0645(02)00021-8.

704 Marty, J.C., Chiavérini, J., Pizay, M.D., Avril B., 2002. Seasonal and interannual
705 dynamics of nutrients and phytoplankton pigments in the western Mediterranean Sea at
706 the DYFAMED time-series station (1991–1999). Deep-Sea Research II 49,1965–1985,
707 doi:10.1016/S0967-0645(02)00022-X.

708 Marty, J.C., Chiavérini, J., 2010. Hydrological changes in the Ligurian Sea (NW
709 Mediterranean, DYFAMED site) during 1995–2007 and biogeochemical consequences.
710 Biogeosciences 7, 2117-2128, doi:10.5194/bg-7-2117-2010.

711 Marty, J.C., Nicolas, E., 1987. Vertical flux of selected organic compounds and trace-
712 metals in the Ligurian Sea. Ann. Inst. Oceanogr. 69, 1, 111-114.

713 Millot, C., 1999. Circulation in the Western Mediterranean Sea. J. Mar. Syst. 20, 423-
714 442, doi:10.1016/S0924-7963(98)00078-5.

715 Migon, C., 2005. Trace metals in the Mediterranean Sea. In: Chemistry of the
716 Mediterranean Sea, A. Saliot (ed.), The Handbook of Environmental Chemistry,
717 Springer, Berlin/Heildelberg (Germany), pp. 151-176.

718 Migon, C., Alleman, L., Leblond, N., Nicolas, E., 1993. Evolution of atmospheric lead
719 in northwestern Mediterranean between 1986 and 1992. Atmos. Environ. 27A, 14,
720 2161-2167, doi:10.1016/0960-1686(93)90045-Z.

721 Migon, C., Nicolas, E., 1998. The trace metal recycling component in the northwestern
722 Mediterranean. Mar. Pollut. Bull. 36, 4, 273-277, doi:10.1016/S0025-326X(98)00160-
723 X.

724 Migon, C., Robin, T., Dufour, A., Gentili, B., 2008. Decrease of lead concentrations in
725 the Western Mediterranean atmosphere during the last 20 years. Atmos. Environ. 42,
726 815-821, doi:10.1016/j.atmosenv.2007.10.078.

727 Migon, C., Sandroni, V., Marty, J.C., Gasser, B., Miquel, J.C., 2002. Transfer of
728 atmospheric matter through the euphotic layer in the northwestern Mediterranean:
729 seasonal pattern and driving forces. Deep-Sea Res. II 49, 2125-2141,
730 doi:10.1016/S0967-0645(02)00031-0.

731 Morel, F.M.M., 2008. The co-evolution of phytoplankton and trace element cycles in
732 the oceans. Geobiol. 6, 318-324, doi:10.1111/j.1472-4669.2008.00144.x.

733 Morel, F.M.M., Price, N.M., 2003. The biogeochemical cycles of trace metals in the
734 oceans. Science 300, 944-947, doi:10.1126/science.1083545.

735 Morley, N.H., Burton, J.D., Tankere, S.P.C., Martin, J.M., 1997. Distribution and
736 behaviour of some dissolved trace metals in the western Mediterranean Sea. Deep-Sea
737 Res. II 44, 675-691, doi:10.1016/S0967-0645(96)00098-7.

738 Moulin, C., Lambert, C.E., Dulac, F., Dayan, U., 1997. Control of atmospheric export
739 of dust from North Africa by the North Atlantic oscillation. Nature 387, 691-4,
740 doi:10.1038/42679.

741 Nicolas, E., Migon, C., Béthoux, J.P., 1998. Oceanic transfer of trace metals by
742 biogenic and lithogenic particles. Mediterranean Targeted Project (MTP II - MATER)
743 3rd Workshop, Rhodos (Greece), 15-17 October 1998, 179-180.

744 Nicolas, E., Ruiz-Pino, D., Buat-Ménard, P., Béthoux, J.P.,1994. Abrupt decrease of
745 lead concentration in the Mediterranean Sea: A response to antipollution policy.
746 Geophys. Res. Lett. 21, 2119-2122, doi:10.1029/94GL01277.

747 Niewiadomska, K., Claustre, H., Prieur, L., D'Ortenzio, F., 2008. Submesoscale
748 physical-biogeochemical coupling across the Ligurian Current (northwestern
749 Mediterranean) using a bio-optical glider. Limnol. Oceanogr. 53, 2210-2225,
750 doi:10.4319/lo.2008.53.5_part_2.2210.

751 Noble, A.E., Echegoyen-Sanz, Y., Boyle, E.A., Ohnemus, D.C., Lam, P.J., Kayser, R.,
752 Reuer, M., Wu, J., Smethie, W., 2015. Dynamicvariability of dissolved Pb and Pb
753 isotope composition from the U.S. North Atlantic GEOTRACES transect. Deep-Sea
754 Res. II 116, 208-225, doi:10.1016/j.dsr2.2014.11.011.

755 Nozaki, Y., 1997. A fresh look at element distribution in the North Pacific Ocean. Eos
756 78, 21, 221-223.

757 Pasqueron de Fommervault, O., Migon, C., D'Ortenzio, F., Ribera d'Alcalà, M.,
758 Coppola, L., 2015. Temporal variability of nutrient concentrations in the northwestern
759 Mediterranean Sea (DYFAMED time-series station). Deep-Sea Res. I 100, 1-12,
760 doi:10.1016/j.dsr.2015.02.006.

761 Passow, U., 2004. Switching perspectives: Do mineral fluxes determine particulate

762 organic carbon fluxes or vice versa? Geochem. Geophys. Geosyst. 5, 5,
763 doi :10.1029/2003GC000670.

764 Ras, J., Claustre, H., Uitz, J., 2008. Spatial variability of phytoplankton pigment
765 distributions in the Subtropical South Pacific Ocean: comparison between in situ and
766 predicted data. Biogeosciences 5, 353-369.

767 Roether, W., Jean-Baptiste, P., Fourré, E., Sültenfuß, J., 2013. The transient
768 distributions of nuclear weapon-generated tritium and its decay product ^{3}He in the
769 Mediterranean Sea, 1952-2011, and their oceanographic potential. Ocean Sci. 9, 837-
770 854, doi:10.5194/os-9-837-2013.

771 Saito, M.A., Moffett J.W., 2002. Temporal and Spatial variability of cobalt in the
772 Atlantic Ocean. Geochim. Cosmochim. Acta, 66, 1943-1953, doi:10.1016/S0016-
773 7037(02)00829-3.

774 Saito, M., Moffett, J.W., 2001. Complexation of cobalt by natural organic ligands in the
775 Sargasso Sea as determined by a new high-sensitivity electrochemical cobalt speciation
776 method suitable for open ocean work. Mar. Chem. 75, 49-68, doi:10.1016/S0304-
777 4203(01)00025-1.

778 Saito, M.A., Noble, A.E., Hawco, N., Twining, B.S., Ohnemus, D.C., John, S.J., Lam,
779 P.J., Conway, T.M., Johnson, R., McIlvin, M.R., 2017. The acceleration of dissolved
780 cobalt's ecological stoichiometry due to biological uptake, remineralization and
781 scavenging in the Atlantic Ocean. Biogeosciences 14, 4637-4662, doi:10.5194/bg-14-
782 4637-2017.

783 Sarthou, G., Jeandel, C., 2001. Seasonal variations of iron concentrations in the
784 Ligurian Sea and iron budget in the Western Mediterranean Sea. Mar. Chem. 74, 115-
785 129, doi:10.1016/S0304-4203(00)00119-5.

786 Schlitzer, R.A., et al., 2018. The GEOTRACES intermediate data product 2017. Chem.
787 Geol. 493, 210-223, doi:10.1016/j.chemgeo.2018.05.040.

788 Schröder, K., Gasparini, G.P., Tangherlini, M., Astraldi, M., 2006. Deep and
789 intermediate water in the Western Mediterranean under the influence of the Eastern
790 Mediterranean Transient. Geophys. Res. Lett. 33, L21607, doi:10.1029/2006gl027121.

791 Seyler, P., Elbaz-Poulichet, F., Guan, D.M., Zhong, X.M., Martin, J.M., 1989.
792 Preliminary results on trace elements distribution in the Gulf of Lions (TYRO cruise,
793 July 1987), Wat. Pollut. Res. Reports 13, 207-222.

794 Shen, G.T., Boyle, E.A., 1988. Thermocline ventilation of anthropogenic lead in the
795 Western North-Atlantic. J. Geophys. Res. 93 (C12), 15715-15732,
796 doi:10.1029/Jc093ic12p15715.

797 Sunda, W.G., Huntsman, S.A., 1995. Cobalt and zinc interreplacement in marine
798 phytoplankton: Biological and geochemical implications. Limnol. Oceanogr. 40, 1404-
799 1417, doi:10.4319/lo.1995.40.8.1404.

800 Tanguy, V., Waeles, M., Gigault, J., Cabon, J.Y., Quentel, F., Riso, R.D., 2011. The
801 removal of colloidal lead during estuarine mixing: seasonal variations and importance
802 of iron oxides and humic substances. Mar. Freshwat. Res. 62, 329– 340,
803 doi:10.1071/MF10220.

804 Tappin, A.D., Hydes, D.J., Burton, J.D., Statham, P.J., 1993. Concentrations,
805 distributions and seasonal variability of dissolved Cd, Co, Cu, Mn, Ni, Pb and Zn in the
806 English Channel. Cont. Shelf Res. 13, 941-969.

807 Testor, P., Bosse, A., Houpert, L., Margirier, F., Mortier, L., Legoff, H., Dausse, D.,
808 Labaste, M., Karstensen, J., Hayes, D., Olita, A., Ribotti, A., Schroeder, K., Chiggiato,
809 J., Onken, R., Heslop, E., Mourre, B., D'Ortenzio, F., Mayot, N., Lavigne, H.,

Pasqueron de Fommervault, O., Coppola, L., Prieur, L., Taillandier, V., Durrieu de Madron, X., Bourrin, F., Many, G., Damien, P., Estournel, C., Marsaleix, P., Taupier-Letage, I., Raimbault, P., Waldman, R., Bouin, M.N., Giordani, H., Caniaux, G., Somot, S., Ducrocq, V., Conan, P., 2018. Multiscale observations of deep convection in the Northwestern Mediterranean Sea during winter 2012-2013 using multiple platforms. J. Geophys. Res. Oceans 123, 1745-1776, doi:10.1002/2016JC012671.

Waeles, M., Riso, R.D., Le Corre, P., 2007. Distribution and seasonal changes of lead in an estuarine system affected by agricultural practices: the Penze estuary, NW France. Est. Coast. Shelf Sci. 74, 570–578, doi:10.1016/j.ecss.2007.05.002.

Waldman, R., Brüggemann, N., Bosse, A., Spall, M., Somot, S., Sevault, F., 2018. Overturning the Mediterranean thermohaline circulation. Geophys. Res. Lett. 45, 8407-8415, doi:10.1029/2018/GL078502.

Wangersky, P.J., 1986. Biological control of trace metal residence time and speciation: A review and synthesis. Mar. Chem. 18, 269-297.

Yoon, Y.Y., Martin, J.M., Cotté, M.H., 1999. Dissolved trace metals in the western Mediterranean Sea: total concentration and fraction isolated by C18 Sep-Pak technique. Mar. Chem. 66, 3-4, 129-148, doi:10.1016/S0304-4203(99)00033-X.

Zhang, X., Xue, Q., Li, L., Fan, E., Wu, F., Chen, R., 2016. Sustainable Recycling and regeneration of Cathode Scraps from Industrial Production of Lithium-Ion Batteries. Sustainable Chem. Eng. 2016, 4, 7041−7049, doi:10.1021/acssuschemeng.6b01948.

Zurbrick, C.M., Boyle, E.A., Kayser, R.J., Reuer, M.K., Wu, J., Planquette, H., Shelley, R., Boutorh, J., Cheize, M., Contreira, L., Menzel Barraqueta, J.L., Lacan, F., Sarthou, G., 2018. Dissolved Pb and Pb isotopes in the North Atlantic from the

GEOVIDE transect (GEOTRACES GA-01) and their decadal evolution.
Biogeosciences 15, 4995-5014, doi:10.5194/bg-15-4995-2018.

Table caption

Table 1: Statistics for trace metal (TM) concentrations measured at the DYFAMED station (Ligurian Sea) from July 2007 to March 2009. Min.: minimum; Max.: maximum; N: number of determinations, SD: standard deviation. The last line of the table indicates the significance level of the difference in TM mean concentrations between surface-100 m and 100 m-bottom layers. T-tests were applied on normally distributed concentrations, i.e. Ni and Cu, whereas non-parametric Mann-Witney tests were performed for Co and Pb (see Fig. S1, in SI, for normality testing). Thus, when distinguishing photic (< 100 m) from deep layer (> 100 m), it appears that mean concentrations were systematically higher in the photic zone for Co, Cu and Pb.

	Co (pM)	Ni (nM)	Cu (nM)	Pb (pM)
		Full water column		
Min. – Max. (N)	28 – 172 (204)	3.57 – 5.52 (200)	1.39 – 2.89 (187)	82 – 235 (130)
Arithmetic mean (SD)	61 (29)	4.54 (0.39)	1.97 (0.28)	117 (24)
Geometric mean (Median)	55 (51)	4.52 (4.58)	1.95 (1.93)	115 (112)
		Surface – 100 m		
Min. – max. (N)	56 – 172 (88)	3.57 – 5.37 (90)	1.39 – 2.89 (81)	90 – 235 (63)
Arithmetic mean (SD)	88 (25)	4.26 (0.34)	2.07 (0.30)	126 (28)
Geometric mean (Median)	85 (81)	4.24 (4.22)	2.05 (2.03)	123 (120)
		100 m – bottom		
Min. – max. (N)	28 – 70 (116)	3.96 – 5.52 (110)	1.39 – 2.60 (106)	82 – 152 (67)
Arithmetic mean (SD)	41 (8)	4.76 (0.25)	1.89 (0.23)	108 (14)
Geometric mean (Median)	40 (39)	4.76 (4.74)	1.88 (1.89)	107 (106)
Significance level	< 0.001	< 0.01	< 0.01	< 0.001

Figure captions

Fig. 1: Location of the DYFAMED sampling site (43° 25'N, 7°52' E), in the Ligurian Sea, with the North Current. The atmospheric time-series station (Cap Ferrat) is located close to Nice (see, e.g., Migon et al., 2008). Figure modified from Heimbürger et al. (2014).

Fig. 2: Temporal evolution of the mixed layer depth (MLD) and total integrated chlorophyll-a (∫TChla) at the DYFAMED site from July 2007 to March 2009.

Fig. 3: Vertical (a) phosphate and (b) silicate concentration profiles (0-2200 m) at the DYFAMED site from July 2007 to March 2009.

Fig. 4: Vertical profiles of trace metals (0-2200 m) at the DYFAMED site from July 2007 to March 2009: a: Co, b: Ni, c: Cu, and d: Pb. Note Co and Pb concentrations are expressed in pM, and Ni and Cu concentrations are expressed in nM.

875 **Figure 1**

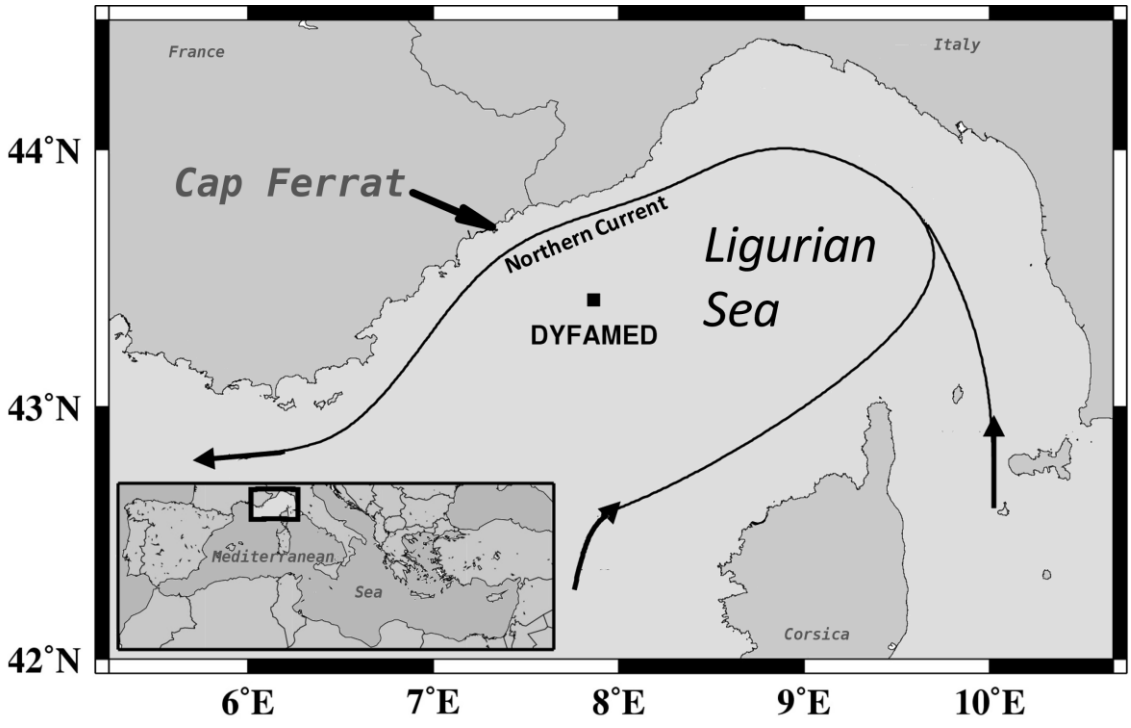

876

877 **Figure 2**

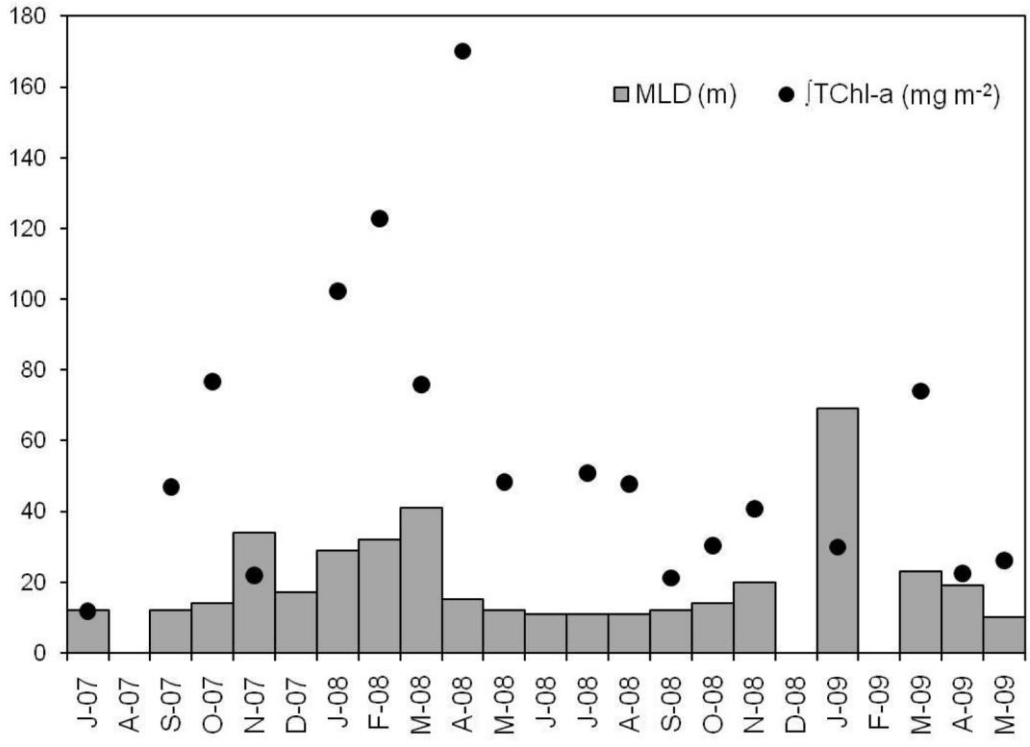

878

Figure 3

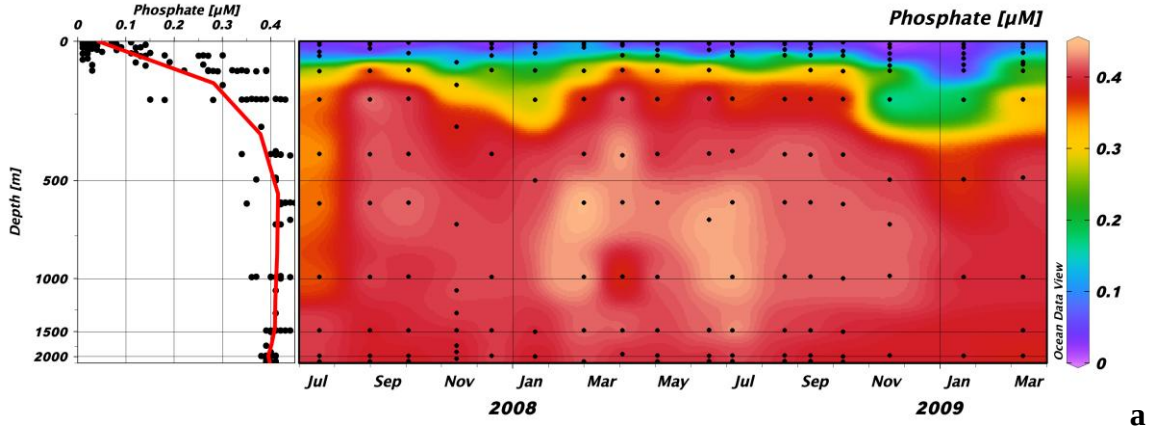
Phosphate [µM]
0
0.1
0.2
0.3
0.4
Depth [m]
0
500
1000
1500
2000
Phosphate [µM]
0.4
0.3
0.2
0.1
0
Ocean Data View
Jul
Sep
Nov
Jan
Mar
May
Jul
Sep
Nov
Jan
Mar
2008
2009

a

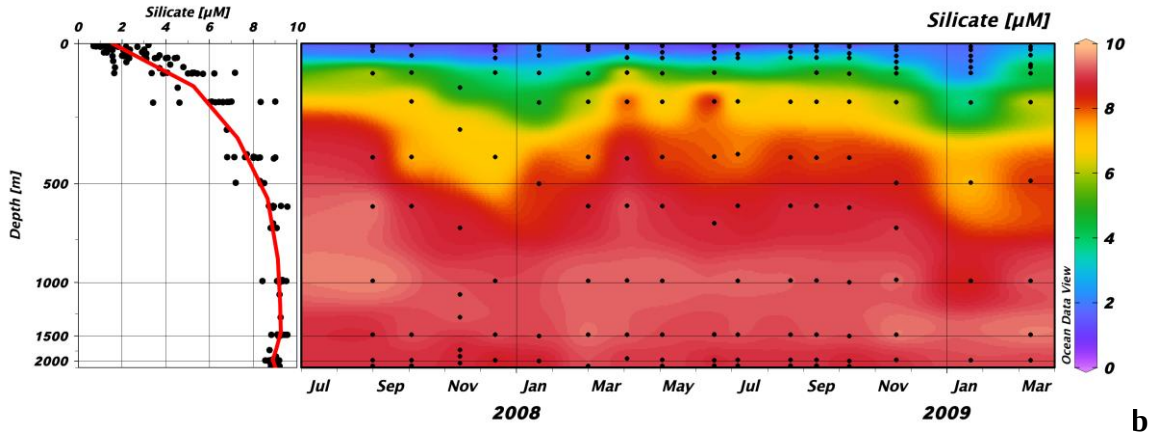
Silicate [µM]
0
2
4
6
8
10
Depth [m]
0
500
1000
1500
2000
Silicate [µM]
10
8
6
4
2
0
Ocean Data View
Jul
Sep
Nov
Jan
Mar
May
Jul
Sep
Nov
Jan
Mar
2008
2009

b

Figure 4

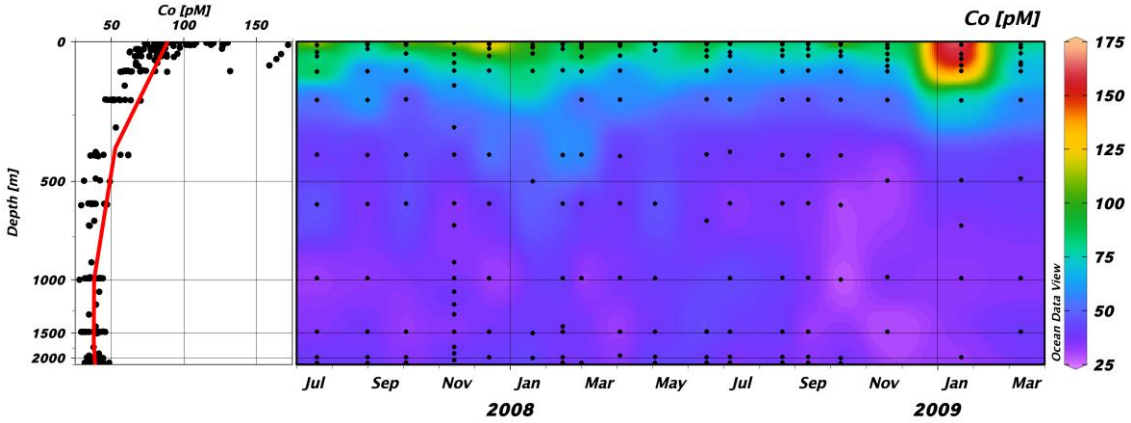
Co [pM]
50
100
150
Depth [m]
0
500
1000
1500
2000
Co [pM]
175
150
125
100
75
50
25
Ocean Data View
Jul
Sep
Nov
Jan
Mar
May
Jul
Sep
Nov
Jan
Mar
2008
2009

a

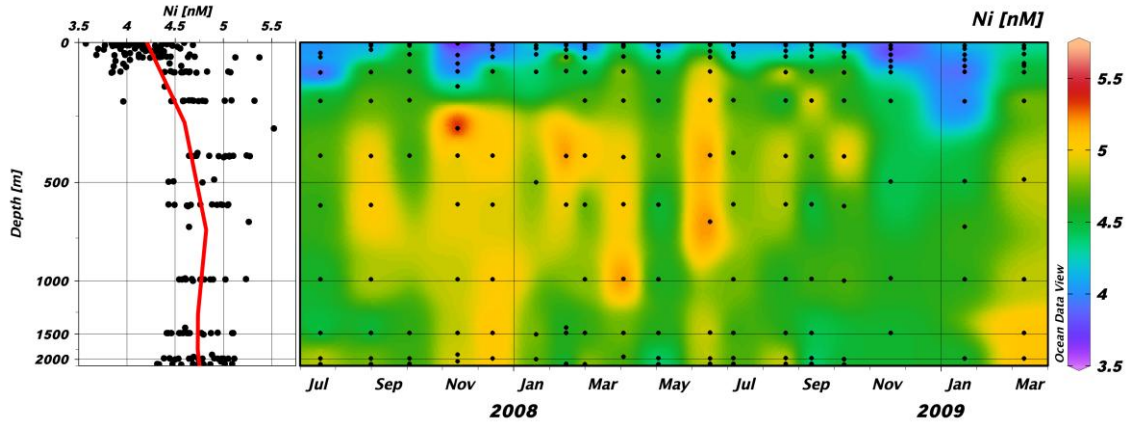
Ni [nM]
3.5
4
4.5
5
5.5
Depth [m]
0
500
1000
1500
2000
Ni [nM]
5.5
5
4.5
4
3.5
Ocean Data View
Jul
Sep
Nov
Jan
Mar
May
Jul
Sep
Nov
Jan
Mar
2008
2009

b

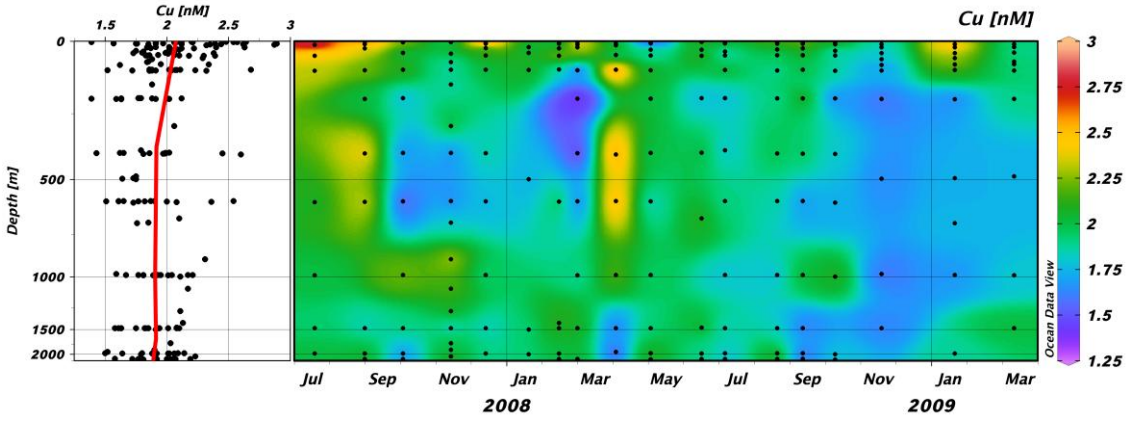
Cu [nM]
1.5
2
2.5
3
Depth [m]
0
500
1000
1500
2000
Cu [nM]
3
2.75
2.5
2.25
2
1.75
1.5
1.25
Ocean Data View
Jul
Sep
Nov
Jan
Mar
May
Jul
Sep
Nov
Jan
Mar
2008
2009

c

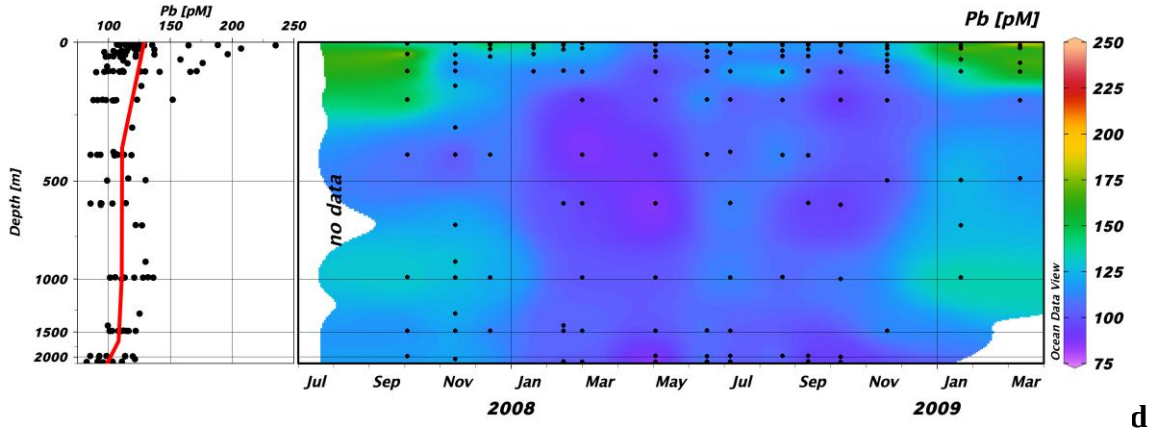
Pb [pM]
100
150
200
250
0
500
1000
1500
2000
Depth [m]
Pb [pM]
250
225
200
175
150
125
100
75
Ocean Data View
no data
Jul
Sep
Nov
Jan
Mar
May
Jul
Sep
Nov
Jan
Mar
2008
2009

d